Compact waveguide bandpass filter employing two-dimensional metallic photonic crystals for millimeter to terahertz frequencies

Feng Lan (兰 峰)[1*], Ziqiang Yang (杨梓强)[1], Limei Qi (亓丽梅)[2], and Zongjun Shi (史宗君)[1]

[1] *School of Physical Electronics, University of Electronic Science and Technology of China, Chengdu 610054, China*

[2] *College of Physics and Engineering, Qufu Normal University, Qufu 273165, China*

[*] *Corresponding author: lanf_uestc@aliyun.com*

Received December 5, 2013; accepted March 5, 2014; posted online April 4, 2014

Two-dimensional metallic photonic crystal slabs with square lattice are proposed to be used for the design of waveguide bandpass filters operating in millimeter to terahertz region. Filter characteristics are studied when rod radii and lattice constants are changed. Based on the frequency scaling technique, a series of higher frequency filters has been designed. By using laser drilling and welding processing techniques, a compact waveguide filter embedded in an EIA-WR10 waveguide with central frequency 145.5 GHz and 3-dB bandwidth of 5.26 GHz is fabricated and measured. The measurement data agree well with the simulation prediction.

OCIS codes: 040.2235, 120.2440, 050.5298, 120.7000.

doi: 10.3788/COL201412.040401.

Millimeter to terahertz (THz) radiations[1,2] have attracted much attention for their special properties[3−5], such as biomedical diagnostics, communications, imaging, and spectroscopy. In recent years, many researches on photonic crystals (PCs) have attracted much attention for the remarkable feature of photonic band gap, which offers a possibility to design new devices[6−10]. The pass band filter is one of the most important devices which can manipulate THz radiations effectively. With the development of THz communication technology, miniaturization has become the new direction of development of the waveguide filter. However, traditional technologies targeting on microwave, infrared or visible light maybe unsuitable or difficult to fabricate bandpass filter for THz region. Metallic photonic crystal filters (MPC) are promising alternatives, and have the advantages of being compact, robust, and inexpensive. Tunable metallic photonic crystal filters composing of two orthogonal linear grids proposed and demonstrated[11,12]. A passband filter which had a dual array structure of the same period but different pillar diameters was fabricated and tested[13]. Recently, a passband filter utilizing the distinction between positive and negative refractions in a metallic photonic crystal prism was studied by the finite difference time domain (FDTD) method[14].

In this letter, the filter characteristics of two-dimensional (2D) metallic photonic crystals are analyzed by varying the radii of metallic rods and lattice constants using the FDTD method and a three-dimensional (3D) full-wave electro-magnetic solver, ansoft HFSS[15].A series of compact waveguide bandpass filters employing 2D metallic photonic crystals for THz range are designed. A prototype of MPC filter with a central frequency of 145.5 GHz and a 3-dB bandwidth of 5.26 GHz is simulated and measured in the region of 100–150 GHz.

Band diagrams provide a quick overview of the most important properties of photonic crystals. Figure 1(a) shows the normalized band diagram of a square lattice MPC obtained by FDTD. Only the first and second TM modes are given along $\Gamma - X$ direction with r and a being the radius and lattice constant and rod ratio $t = r/a$=0.26. It can be seen that the first mode shows a passband characteristic, if selecting a=1.43 mm. The passband frequency varies from 128 to 142 GHz.

The simulation model is symmetrical along the center rods which are named as rod "1", "2", and "3", with rod ratios $t_1 = t_2 = t_3$=0.26, respectively, as is shown in Fig. 1(b). The number of rods of a single lattice is expressed as N_y, and N_y=5. The box is defined as air material with width $L_x = a$, length $L_y = 5a$, and height $L_z = 0.5a$. The rod is defined as perfect metal with radius $r = 0.26a$. As for boundary conditions[16], the yz and xy planes on each side of the box are assumed to be perfect magnetic conductor (PMC) and perfect electric conductor (PEC), respectively, and the xz planes are set as waveports.

In order to achieve the fundamental structure of a band pass filter with central frequency 145 GHz, optimization of rod ratios and MPC periodicity N_y toward the transmission direction in a single slab is performed

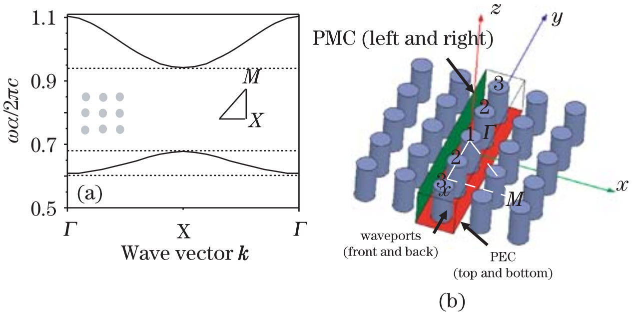

Fig. 1. (a) Band diagram of the first and second modes along $\Gamma - X$ direction. (b) Simulation model for metallic TM photonic crystals.

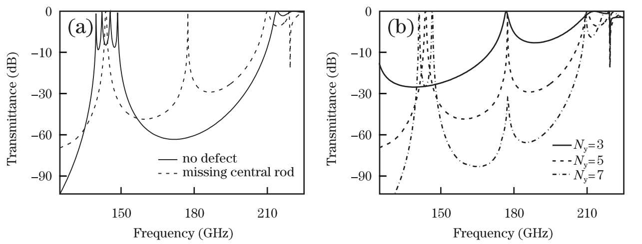

Fig. 2. (a) Transmission spectra of MPC for no defect (solid line) and one central rod missing (dashed line). (b) Transmission spectra of MPC with defection for different numbers of layers.

firstly. Transmission spectra for five-layer MPC with the same rod ratios are shown in Fig. 2(a). The transmission curve of the solid line represents MPC without defects, as t_1=0.26. It is found that there is a wide pass band corresponding to the first mode. Four ripples caused by Bragg scattering are strong and their magnitudes reach to −20 dB in the band. Band region of the first mode varies from 135 to 150 GHz with about 7 GHz offset than that of the FDTD results for different theoretic models. For FDTD calculations, MPC is a perfect 2D model, while it is a 3D model with five rods in transmission direction for HFSS simulation. Nonetheless the band diagram of FDTD results would give a first direction for the design of a simulation model. The dotted line represents the transmission spectrum of MPC when the central rod is removed, as t_1=0. It is found that two narrow pass bands appear. One is around 145 GHz for the first mode and the other one appears around 177 GHz in the gap of two previous modes.

MPC would possess filter characteristics when appropriate defects are made. When the central rod is removed, Fig. 2(b) shows the transmission spectra of MPC with three-layer, five-layer, and seven-layer toward the transmission direction. In the original region of the first mode, for N_y=3, there is no pass band; for N_y=7, a pass band with two deep ripples appears, which is unfavorable for widespread band filtering. In the original gap region, a pass band exists for every structure. For N_y=3, the outer band attenuation is smaller on the high frequency band. For N_y=7, the pass band attenuation is too large so that it exceeds 40 dB. Therefore, the five-layer MPC is more suitable for forming a narrow band filter with two pass bands.

By using the Multiple Multipole Program combined with Model-Based Parameters Estimation technique, Cui *et al*. have proposed to design metallic-dielectric photonic crystal filters at optical frequency by optimizing rod radii[17,18]. In the following, we intend to study the filter characteristics of five-layer MPC by changing the rod radii.

The transmission spectra of MPC by changing the rod ratio $t_2 = r_2/a$ and $t_3 = r_3/a$ simultaneously are shown in Fig. 3(a). The solid, dotted, and dot-dash lines denote $t_2 = t_3$=0.2, 0.15, and 0.1, respectively. It can be seen that with $t_2 = t_3$ decreasing simultaneously, the band shifts to a lower frequency and band ripples diminish. When $t_2 = t_3$=0.1, a wider pass band with the central frequency of 117 GHz and the 3-dB width of 2 GHz occurs. Now, by only varying t_3 while keeping t_1=0.26 and t_2=0.15 constant, transmission spectra of MPC are shown in Fig. 3(b). The solid, dotted, and dot-dash lines denote t_3=0.15, 0.1, and 0.05, respectively. One can see that the band moves toward a lower frequency with the decreasing band width and ripples as t_3 decreases. While t_3=0.05, a band pass with a central frequency of 115 GHz and the 3-dB width of 2.1 GHz appears.

Figure 3(c) shows transmission characteristics of MPC by changing t_1 while keeping t_2=0.15 and t_3=0.05 constant. The solid, dotted, and dot-dash lines denote t_1=0.26, 0.23, and 0.2, respectively. When t_1 is decreasing, a wider pass band filter at a low frequency is obtained, and stronger ripples appear. Assuming t_1=0.2, t_2=0.08, and t_3=0.06, a wide pass band filter with a central frequency of 106 GHz and the 3-dB band width of 5.8 GHz is obtained as shown in Fig. 3(d).

By using the scaling properties for photonic crystal[19], one could design a series of THz pass band filters. If decreasing or increasing the rod radii while keeping rod ratio unchanged, the pass band would shift to higher or lower frequency, respectively. Furthermore, one can easily obtain desired bandwidth by tuning the rod ratios. However, the filter characteristics would not remain the same unless one only changes the lattice constant and rod radii but keeps the rod ratios fixed.

Three pieces of single 5-layer slab MPC were cascaded to form a waveguide filter. The layout of the filter design is illustrated in Fig. 4(a). It is a 3×5 array of metal rods lying on a square lattice. Fifteen metal rods were

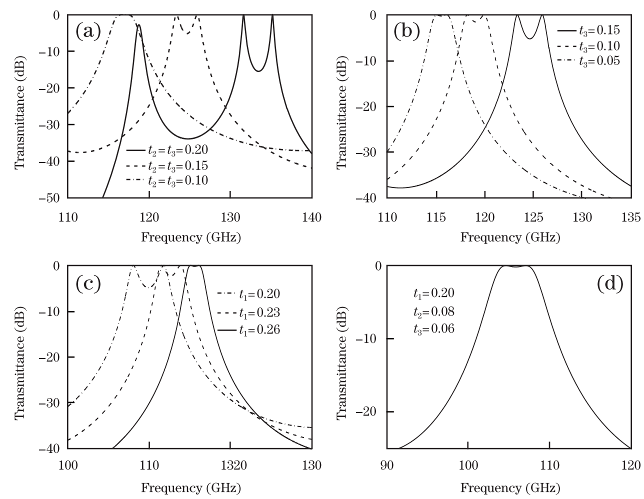

Fig. 3. Transmission spectra of MPC by changing rods parameters with 5 layers and lattice constant a=1.43 mm. (a) By changing rod "2" and "3" simultaneously; (b) by changing rod "3" only; (c) by changing rod "1" only; (d) by changing rod "1", "2", and "3", respectively.

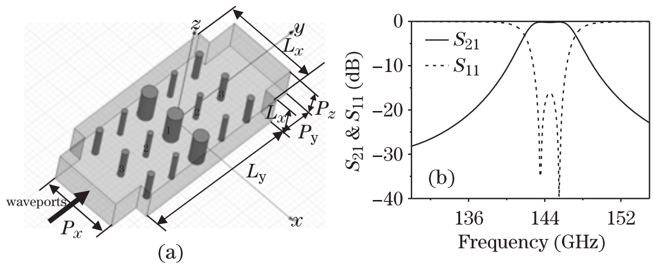

Fig. 4. (a) Simulation model of MPC waveguide filters. (b) Transmission and reflection spectra of MPC waveguide filters.

Table 1. Geometrical Parameters for MPC Filter

Parameters	(mm)
Lattice Constant	a=1.16
Radius of Rod "1"	r_1=0.2725
Radius of Rod "2"	r_2=0.1025
Radius of Rod "3"	r_3=0.115
Width of the Filter	$L_x = 3a$=3.48
Length of the Filter	$L_y = 5a$=5.8
Length of Wave Ports	$P_y = a$=1.16
Wider Side of Wave Ports	P_x=2.54
Narrow Side of Wave Ports	P_z=1.27

embedded in a rectangular cavity linked with a particular rectangular waveguide. All the metal rods were divided into three groups. Group 1 of 3 pillars was located in the middle of the filter cavity and group 2 and group 3 of 6 pillars were symmetric relative to group 1, respectively.

Parameters of the waveguide filter are given in Table 1. Square lattice constant a=1.16 mm. Radii of rods "1", "2" and "3" are r_1=0.2725 mm, r_2=0.1025 mm, and r_3=0.115 mm, respectively. Filter cavity width, length, and height are $L_x = 3a$=3.48 mm, $L_y = 5a$=5.8 mm and L_z=1.27 mm, respectively. Waveports are normal EIA-WR10 ports with P_x=2.54 mm, P_z=1.27 mm, and length P_y=a=1.16 mm. Figure 4(b) gives the simulation results where the solid and dotted lines denote the transmission and reflection spectra, respectively. It can be seen that there is a pass band with a central frequency of 145.5 GHz and the bands of 141.94-147.20 GHz. The maximum loss in the pass band region is less than 0.15 dB.

A series of THz bandpass filters from 110 GHz to 1 THz have been designed by scaling the present filter design accordingly. The dimensions of these filters can be determined by the scale factors related to wavelength of the center frequency: λ/a=1.784, λ/r_1=7.593, λ/r_2=20.185 and λ/r_3=17.990. Figure 5 shows several designs of MPC filter working at the frequencies of 220, 291, 340, 420, and 500 GHz. These filters were embedded in the standard rectangular waveguides of EIA-WR6, WR5, WR4, and WR3. By changing lattice constant a and rod raius "r_1", "r_2" and "r_3" and keeping rod ratios unchanged, the center frequency shifts toward higher or lower frequencies with almost the same bandwidth and insertion loss.

The waveguide filter was produced by traditional mechanical operations. At the beginning, two flimsy steel plates with similar array holes were fabricated by laser beam machining, followed by plating with gold. The varied gilt rods were manufactured by coating removal enamelled wires. The filter cavity was divided into two symmetrical plates. Then the filtering parts were mounted on the recombined cavity plates with several locating dowels. At the end we welded the gilt wires to the gilt flimsy plates, and embedded the filtering structure in the waveguide. Figure 6(a) shows two metallic flimsy plates and Fig. 6(b) shows the fabricated MPC filter parts where gilt rods are sealed with cavity parts between the plates. Four dowels around the filter cavity were used to fix the MPC in a metallic shell. Two parts of the metallic shell and the whole outlook drawing of the shell are shown in Fig. 6(c) and 6(d), respectively.

Figure 7(a) shows the experiment setup for the measurement of S_{21} with a backward wave oscillator (BWO) as source and a broadband power meter. In Fig. 7(a) no. 1, 2, 3, 4 and 5 represent BWO, BWO voltage modulator, power meter probe, power meter and filter respectively. The BWO output frequencies can be adjusted by the cathode voltage modulator. As shown in inset of Fig. 7(b), the output frequencies are approximately linear with respect to the voltages. In order to match with the power meter probe and BWO output waveguide, two WR28-WR10 waveguide converters were adopted to connect the filter with probe and output waveguide. To measure the transmission characteristic of MPC filter, we firstly obtained the output power P_1 at different input voltages when filter was absent. Then we got the output power P_2 with the filter at the same input voltages. Transmission spectra could be obtained through equation S_{21}=10 log (P_2/P_1).

The measurement results (circle-solid line) along with simulation results (solid line) are shown in Fig. 7(b). One can see that the trend of the measurement is in agreement with the simulation results; however, the attenuation of experiments is larger. The measured central frequency is 145 GHz, with a minor frequency offset (0.5 GHz). The insertion loss around the measured central frequency is 2.9 dB. The large attenuation is mainly caused by non-

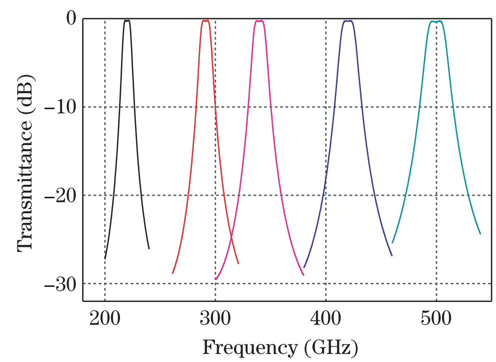

Fig. 5. (Color online) Simulated transmittance of frequency scaled MPC filters.

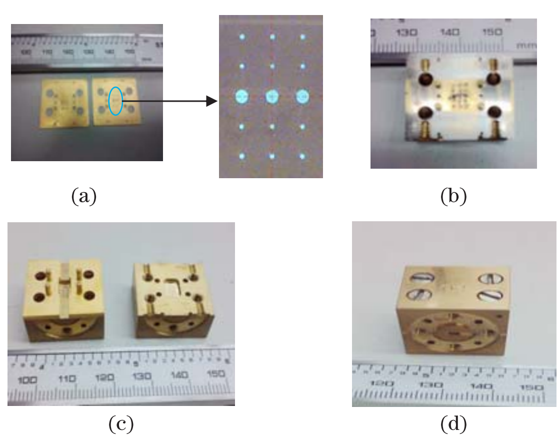

Fig. 6. Image of the fabricated MPC filter and its metallic shell: (a) metallic flimsy plates, (b) fabricated MPC filter parts, (c) two parts of the metallic shell, and (d) outlook drawing of the metallic shell.

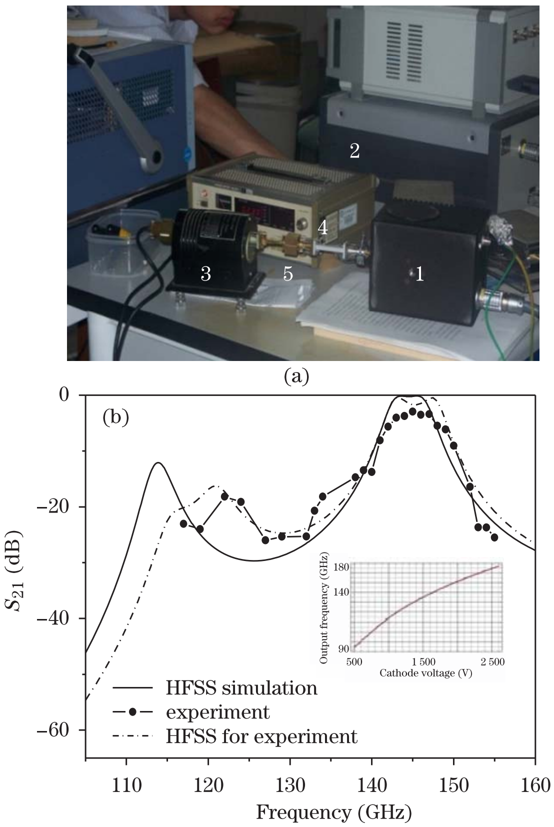

Fig. 7. (a) Experimental setup to measure S_{21}. (b) Simulation and measurement results for the compact bandpass filter.

ideal sample fabrication and mismatching between joints of the waveguides. The bandpass filter shows a big offset of first band region, exactly as predicted by simulation for machining and assembling tolerances. The calculated transmission spectrum (dot-dash line) fits the measured line much better if the rods deviations are considered. The actual rod radii are r_1=0.255 mm, r_2=0.1275 mm, and r_3=0.1225 mm. The rods offset distances of X and Y axes are (0 mm, –0.06 mm), (0 mm, –0.005 mm), and (0 mm, –0.02 mm), respectively. The experiment results accord with the analysis. The truth is that as rod radii decrease or increase while lattice constant remains the same, pass band region tends to shift toward lower frequencies or higher frequencies.

In conclusion, filter characteristics of MPC are studied in this letter. It is found that two narrow pass bands appeared when the central rod is removed for five-layer structure. By decreasing or increasing rod radii, while keeping the rod ratio fixed, the pass band would shift to higher or lower frequencies, respectively. Furthermore, one can improve the bandwidth and attenuation slope by tuning the rod ratios. A series of THz waveguide filters with almost identical bandwidth and attenuation are designed by changing the lattice constant and rod radii and keeping rod ratios unchanged. Therefore, desired passband waveguide filters with desired central frequency and bandwidth can be obtained by optimizing radii of the rods with a reasonable lattice constant. Finally, a compact passband waveguide filter with a central frequency of 145.5 GHz and a bandwidth of 5.26 GHz is fabricated and measured. The measured results are in accordance with the simulation results. The MPC waveguide filter with compact and robust chip structure, inexpensive and easy fabrication features has great application value at THz communication and radar systems.

This work was supported by the National Natural Science Foundation of China (No. 11075032) and the National High Technology Research and Development Program of China (No. 2011AA010204).

References

1. B. Ferguson and X. Zhang, Nat. Mater. **1,** 26 (2002).
2. Z. Zheng, S. Lu, Y. Li, L. Chen, and S. Wen, Chin. Opt. Lett. **10,** 100605 (2012).
3. S. Komiyama, O. Astafiev, V. Antonov, T. Kutsuwa, and H. Hirai, Nature **403,** 405 (2000).
4. X. Zhao, Q. Zhu, and Y. Zhang, Chin. Phys. B **18,** 2864 (2009).
5. K. Ostmann, K. Pierz, G. Hein, P. Dawson, and M. Koch, Electron. Lett. **40,** 124 (2004).
6. M. Tokushima and H. Yamada, IEEE J. Quantum Electron. **38,** 753 (2002).
7. S. Feng and Y. Wang, Chin. Phys. B **20,** 104207 (2011).
8. W. Sun, Y. Liu, D. Wang, L. Han, X. Guo, and Z. Yu, Chin. Phys. B **22,** 014201 (2013).
9. L. Huang, B. Chen, Y. Li, and C. Liu, Chin. Opt. Lett. **10,** 011301 (2012).
10. S. R. Dastjerdi, M. Ghanaatshoar, and T. Hattori, Chin. Opt. Lett. **11,** 102303 (2013).
11. T. D. Drysdale, R. J. Blaikie, and D. R. S. Cumming, J. Appl. Phys. Lett. **83,** 5362 (2003).
12. T. D. Drysdale, I. S. Gregory, C. Baker, E. H. Linfield, W. R. Tribe, and D. R. S. Cumming, J. Appl. Phys. Lett. **85,** 5173 (2004).
13. A. J. Gallant, M. A. Kaliteevski, D. Wood, M. C. Petty, R. A. Abram, S. Brand, G. P. Swift, D. A. Zeze, and J. M. Chamberlain, J. Appl. Phys. Lett. **91,** 161115 (2007).
14. M. A. Kaliteevski, S. Brand, C. J. Garvie, R. A. Abram, and J. M. Chamberlain, Opt. Express **16,** 7330 (2008).
15. HFSS v9, *Getting Started with HFSS* (Ansoft Corporation, Pittsburgh PA, 2004).
16. J. D. Shumpert, W. J. Chappell, and L. P. B. Katehi, J. IEEE Trans. Microwave Theory Technol. **47,** 2099 (1999).
17. X. Cui, C. Hafner, and R. Vahldieck, Opt. Express **13,** 6175 (2005).
18. X. Cui, C. Hafner, K. Tavzarashvili, and R. Vahldieck, J. Opt. Soc. Am. A **24,** 1761 (2007).
19. J. D. Joannopoulos, S. G. Johnson, J. N. Winn, and R. D. Meade, *Photonic Crystals-Molding the Flow of Light* (Princeton University Press, Princeton, 2008).